Glycobiology, 2017, vol. 27, no. 8, 726–733
doi: 10.1093/glycob/cwx045
Advance Access Publication Date: 1 June 2017
Original Article

OXFORD

Chemical Biology

Chemo-enzymatic synthesis of lipid-linked $GlcNAc_2Man_5$ oligosaccharides using recombinant Alg1, Alg2 and Alg11 proteins

Ana S Ramírez[2], Jérémy Boilevin[3], Chia-Wei Lin[4], Bee Ha Gan[3], Daniel Janser[2], Markus Aebi[4], Tamis Darbre[3], Jean-Louis Reymond[3], and Kaspar P Locher[2,1]

[2]Department of Biology, Institute of Molecular Biology and Biophysics, Eidgenössische Technische Hochschule (ETH), Schafmattstrasse 20, CH-8093 Zürich, Switzerland, [3]Department of Chemistry and Biochemistry, University of Berne, CH-3012 Berne, Switzerland, and [4]Institute of Microbiology, Eidgenössische Technische Hochschule (ETH), CH-8093 Zürich, Switzerland

[1]To whom correspondence should be addressed: Tel: +41-44-633-3991; Fax: 41-44-633-1182; e-mail: locher@mol.biol.ethz.ch

Received 3 March 2017; Revised 10 May 2017; Editorial decision 10 May 2017; Accepted 27 May 2017

Abstract

The biosynthesis of eukaryotic lipid-linked oligosaccharides (LLOs) that act as donor substrates in eukaryotic protein N-glycosylation starts on the cytoplasmic side of the endoplasmic reticulum and includes the sequential addition of five mannose units to dolichol-pyrophosphate-$GlcNAc_2$. These reactions are catalyzed by the Alg1, Alg2 and Alg11 gene products and yield Dol-PP-$GlcNAc_2Man_5$, an LLO intermediate that is subsequently flipped to the lumen of the endoplasmic reticulum. While the purification of active Alg1 has previously been described, Alg11 and Alg2 have been mostly studied in vivo. We here describe the expression and purification of functional, full length Alg2 protein. Along with the purified soluble domains Alg1 and Alg11, we used Alg2 to chemo-enzymatically generate Dol-PP-$GlcNAc_2Man_5$ analogs starting from synthetic LLOs containing a chitobiose moiety coupled to oligoprenyl carriers of distinct lengths (C_{10}, C_{15}, C_{20} and C_{25}). We found that while the addition of the first mannose unit by Alg1 was successful with all of the LLO molecules, the Alg2-catalyzed reaction was only efficient if the acceptor LLOs contained a sufficiently long lipid tail of four or five isoprenyl units (C_{20} and C_{25}). Following conversion with Alg11, the resulting C_{20} or C_{25} -containing $GlcNAc_2Man_5$ LLO analogs were successfully used as donor substrates of purified single-subunit oligosaccharyltransferase STT3A from *Trypanosoma brucei*. Our results provide a chemo-enzymatic method for the generation of eukaryotic LLO analogs and are the basis of subsequent mechanistic studies of the enigmatic Alg2 reaction mechanism.

Key words: lipid-linked oligosaccharide, mannosylation, mannosyltransferase, *N*-glycans

Introduction

During protein N-glycosylation, glycans from lipid-linked oligosaccharides (LLOs) are transferred onto asparagine residues located in N-glycosylation sequons (Breitling and Aebi 2013). In eukaryotes, the transferred glycan contains the conserved core $GlcNAc_2Man_5$, while a higher diversity in the chemical structure of the glycans is observed in bacteria and archaea (Dell et al. 2010; Nothaft and Szymanski 2010; Jarrell et al. 2014). In eukaryotes, the synthesis of

LLO comprises three steps: It begins with the biosynthesis of the intermediate Dol-PP-$GlcNAc_2Man_5$, which occurs on the cytoplasmic side of the endoplasmic reticulum (ER). The second step is the flipping of this intermediate to the luminal side of the ER. The third step comprises the glycan extension in the ER lumen, yielding Dol-PP-$GlcNAc_2Man_9$ (Man9). In most eukaryotes, there is an addition of three glucose units to generate Dol-PP-$GlcNAc_2Man_5Glc_3$ (Aebi 2013).

The topic of this study is the biosynthesis of Dol-PP-$GlcNAc_2Man_5$, which starts in the cytoplasm with the addition of N-acetylglucosamine-phosphate (GlcNAc-P) to the phosphorylated lipid carrier dolichol (Dol-P) by the GlcNAc-P transferase, Alg7 (Kukuruzinska et al. 1994). The second GlcNAc unit is added by the Alg13/14 complex, generating Dol-PP-$GlcNAc_2$ (Gao et al. 2008; Lu et al. 2012). Subsequently, five mannose residues are added by the Alg1, Alg2 and Alg11 proteins, proposed to form a complex in the ER membrane (Gao et al. 2004). Alg1 adds a single mannose forming a β-1,4 glycosidic bond (Couto et al. 1984). Alg2 produces the first branch in the core glycan of the eukaryotic N-glycosylation LLO by adding two mannose units to the β-linked mannose added by Alg1, generating α-1,3 and α-1,6 glycosidic linkages (Yamazaki et al. 1998; Takeuchi et al. 1999; Kämpf et al. 2009). The intriguing dual-specificity reaction mechanism of Alg2 is not understood to date, which is in part due to the difficulties associated with the purification of labile membrane proteins such as Alg2 as well as the lack of sufficient amounts of lipid-linked $GlcNAc_2Man$ substrate needed to perform detailed kinetic analyses. The cytoplasmic biosynthesis of the LLO is terminated by the action of Alg11 that catalyzes the addition of two α1,2-linked mannoses to the 1,3-linked mannose added by Alg2 (Cipollo et al. 2001; O'Reilly et al. 2006; Absmanner et al. 2010). After translocation of Dol-PP-$GlcNAc_2Man_5$, further extension of the oligosaccharide is carried out in the lumen of the ER where Dol-P-Man and Dol-P-Glc, respectively, act as substrates for membrane-embedded glycosyltransferases (Burda and Aebi 1999).

In *Trypanosoma brucei*, luminal biosynthesis proceeds to the Dol-PP-$GlcNAc_2Man_9$ stage, but either lipid-linked $GlcNAc_2Man_5$ or $GlcNAc_2Man_9$ glycans are used as substrates in protein N-glycosylation, catalyzed preferentially by the single-subunit OST enzymes TbSTT3A or TbSTT3B, respectively (Manthri et al. 2008; Izquierdo et al. 2009, 2012). This substrate preference has only been studied in vivo, the unavailability of sufficient amounts of pure LLOs has prevented detailed kinetic studies. We have previously reported the expression and purification of TbSTT3A as well as its characterization with LLO analogs composed by chitobiose coupled to oligoprenyl carriers of different lengths (Ramírez et al. 2017). Here, we describe the preparation of LLO analogs with elongated glycan moieties by biochemical addition of mannose units using recombinantly expressed and purified Alg1, Alg2 and Alg11, in analogy to the early steps of the biosynthesis of the eukaryotic native LLO. The generated LLO analogs were fully functional substrates for purified TbSTT3A in in vitro glycosylation assays.

Results

Expression and purification of CT-Alg1, Alg2 and CT-Alg11

In vitro preparation of a dolichol-linked $GlcNAc_2Man_5$ LLO had previously been performed by reaction of Dol-PP-$GlcNAc_2$ with Alg1 expressed and purified from yeast and with membranes from *Escherichia coli* expressing full length Alg2 and Alg11 (O'Reilly et al. 2006). However, neither the Alg2 and Alg11 enzymes nor the resulting $GlcNAc_2Man_5$-containing LLO had been purified for that study. For our structural and functional investigations of the Alg pathway as

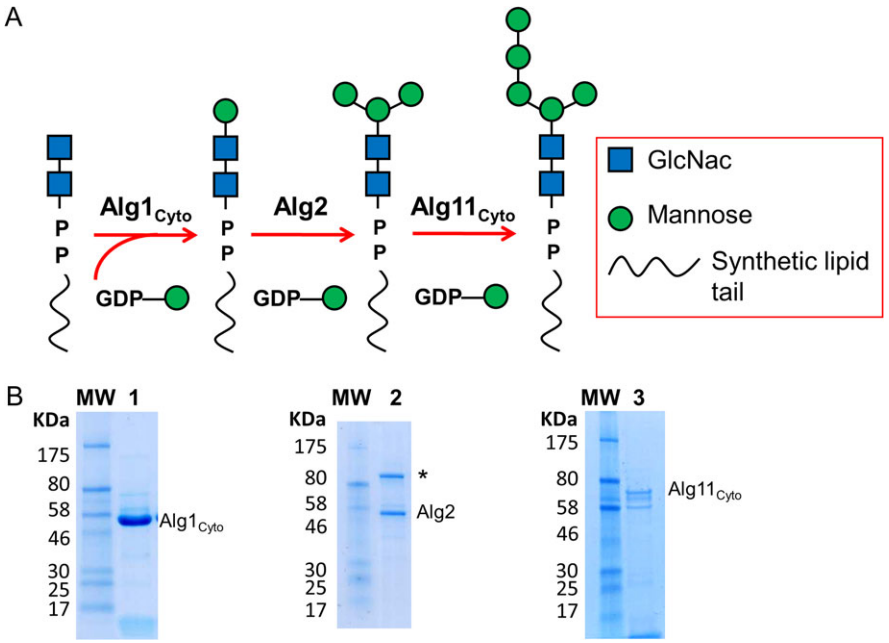

Fig. 1. (**A**) Schematic of chemo-enzymatic synthesis strategy to extend the glycan moiety of synthetic LLO analogs to Dol-PP-$GlcNAc_2Man_5$. $Alg1_{Cyto}$ refers to His10-zz-TEV-Alg1(aa 33–349); Alg2 refers to His10-YFP-3C-Alg2 and $Alg11_{Cyto}$ refers to His10-zz-TEV-Alg11(aa 46–548). (**B**) SDS–PAGE analysis of the purified $Alg1_{Cyto}$ (lane 1), Alg2 (lane 2) and $Alg11_{Cyto}$ (lane 3). MW refers to marker proteins, with molecular masses indicted on the side. The asterisk depicts an impurity that co-eluted during Alg2 purification. This figure is available in black and white in print and in color at *Glycobiology* online.

well as for bioengineering purposes, working with the native dolichol is challenging due to the low solubility and the limited amounts that can be generated or obtained. Additionally, working with membrane preparations instead of purified proteins necessitates more and challenging purification steps of the reaction products ($GlcNAc_2Man_5$-LLOs). To overcome these difficulties, we expressed and purified active Alg1, Alg2 and Alg11 proteins, which were used to sequentially add five mannose units to synthetic LLOs bearing a chitobiose moiety coupled to polyprenyl tails of different length (Figure 1A).

The topologies of the yeast Alg1 and Alg11 membrane proteins are similar. Both proteins contain a single, N-terminal transmembrane helix followed by a cytoplasmic, C-terminal domain that harbors the catalytic activity. It was shown earlier that cell extracts of *E. coli* expressing only the cytoplasmic domain of Alg1 could add one mannose residue to Dol-PP-$GlcNAc_2$ in vitro (Couto et al. 1984). Based on these findings, we expressed and purified the cytoplasmic domain of Alg1 ($Alg1_{Cyto}$, aa 33–349) and Alg11 ($Alg11_{Cyto}$, aa 46–548), both fused to a His10-zz-TEV tag to their N-terminus. Both domains showed to be strongly associated with the cell membrane of *E. coli*, and could only be extracted after incubation with detergent (0.5% Triton X-100). These observations agreed with a previous report suggesting that the soluble domain of Alg11 contains two hydrophobic or amphipathic helices in addition to its transmembrane helix, strengthening its association with the ER membrane (Absmanner et al. 2010). We succeeded in purifying both proteins, although sodium dodecyl sulphate–polyacrylamide gel electrophoresis (SDS–PAGE) analysis of Alg11 showed additional bands corresponding to degradation products as confirmed by mass spectrometry (MS) analysis (data not shown). However, these did not negatively affect the catalytic activity of Alg11 (Figure 1B).

The yeast Alg2 protein has a very different topology compared to Alg1 or Alg11. Alg2 consists of two transmembrane helices at the

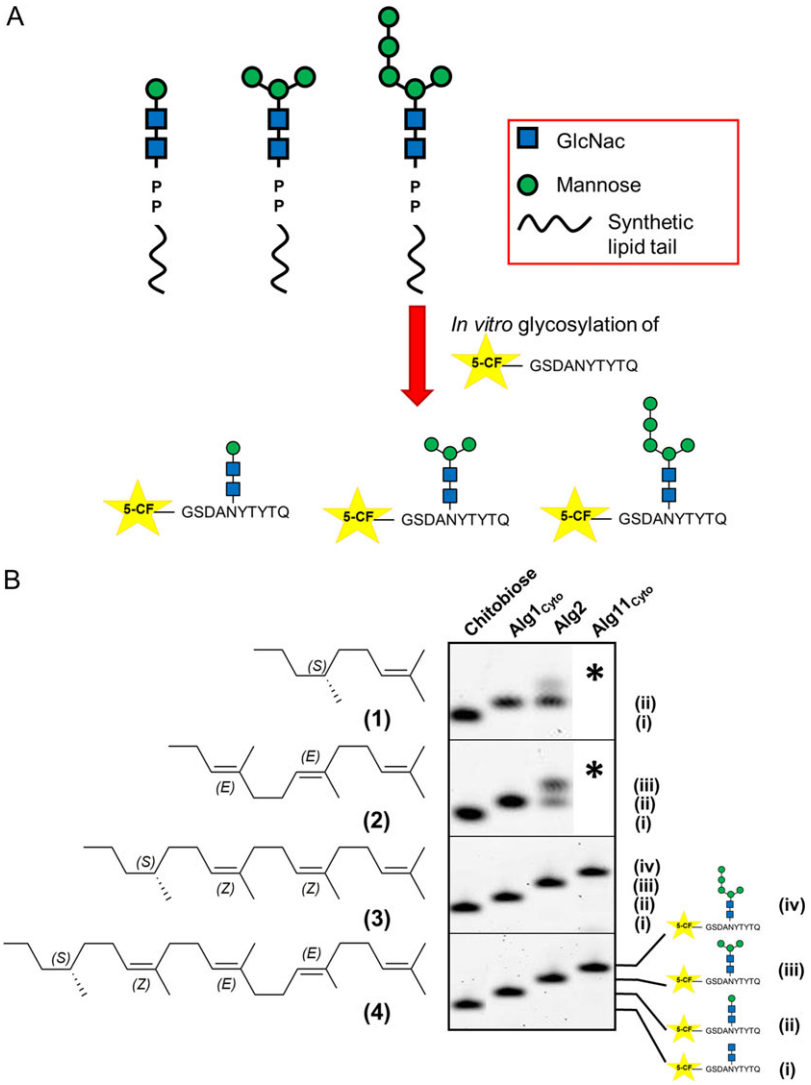

Fig. 2. (**A**) Schematic of product analysis of the Alg protein reactions. The glycans from chemo-enzymatically generated LLO analogs were transferred onto the fluorescently labeled peptide 5CF-GSDANYTYTQ by in vitro glycosylation using purified TbSTT3A protein. Glycopeptides were subsequently analyzed by Tricine SDS–PAGE and LC–MS/MS. (**B**) Tricine SDS–PAGE analysis of glycopeptides produced from LLO analogs with different lipid tails after processing with $Alg1_{Cyto}$, Alg2 and $Alg11_{Cyto}$. (**1**) (*S*)-Citronellyl, C_{10}; (**2**) Farnesyl, C_{15}; (**3**) (*S*)-NerylCitronellyl, C_{20}; (**4**) (*S*)-FarnesylCitronellyl, C_{25}. *Reaction with Alg11 was not performed for the LLOs containing lipids **1** and **2** because the preceding reaction with Alg2 was not successful. LC–MS/MS, liquid chromatography–tandem mass spectrometry. This figure is available in black and white in print and in color at *Glycobiology* online.

N-terminus, followed by a cytoplasmic domain and another two hydrophobic segments at the C-terminus, which were proposed to strongly contribute to its association to the ER membrane (Kämpf et al. 2009). Our attempts to express and purify yeast Alg2, which included transient transfection in human cells and baculovirus-driven expression in insect cells, were unsuccessful. We then focused on the human Alg2 homolog, which in contrast to the yeast protein contains a single transmembrane helix and a cytoplasmic domain (Supplementary Figure 1). Several parameters for the recombinant expression of full length human Alg2 in HEK293 cells were optimized, including the location of the affinity tags tested and the choice of detergent used to solubilize and purify the protein. Screening was aided by the use of fluorescence size exclusion chromatography (Supplementary Figure 2). We obtained best results with an Alg2 construct containing a His_{10}-YFP-3c tag fused to its N-terminus. SDS–PAGE analysis showed that the produced protein was pure (Figure 1B). A second band at higher mass was identified by MS analysis as an impurity, but this contaminant did not affect the catalytic activity of Alg2.

Chemo-enzymatic synthesis of $GlcNAc_2Man_5$ LLO analogs

The preparation of $GlcNAc_2Man_5$ LLO analogs using the purified Alg proteins was pursued starting from synthetic LLO analogs that contained a chitobiose moiety coupled to polyprenyl tails of different length, which had been characterized by MS and nuclear magnetic resonance analyses previously (Figure 2 and Ramírez et al. 2017). We indirectly analyzed the addition of mannose units using the generated LLO analogs as donor substrates for transfer onto fluorescently labeled peptides using purified single-subunit oligosaccharyltransferase TbSTT3A (Ramírez et al. 2017). The resulting glycopeptides were then analyzed by SDS–PAGE tricine gels and by liquid chromatography–tandem mass spectrometry (LC–MS/MS) to identify the glycans attached to them (Figure 2A).

Addition of the first mannose moiety using purified $Alg1_{cyto}$ was successful with all four LLO analogs tested. A shift to higher mass was observed in SDS–PAGE tricine gels for the glycopeptide carrying the additional mannose unit, compared to glycopeptide that only contained chitobiose (Figure 2B). LC–MS/MS analysis confirmed only one product after glycosylation of the peptide with the LLOs originated from the reaction with Alg1, with a molecular weight that corresponds to the peptide linked to $GlcNAc_2Man$ (Figure 3 and Table I). The result was identical for the four polyprenyl tails tested.

The addition of the next two mannoses by Alg2 was successful only with LLO analogs carrying the longer polyprenyl tails (**3**, C_{20} and **4**, C_{25}). For the LLO analogs with shorter lipid tails (**1**, C_{10} and **2**, C_{15}), the reaction with Alg2 was not complete (Figure 2B). LC–MS/MS analyses of the glycopeptides originated from LLOs produced by Alg2, allowed us to identify the reaction products for each LLO analog (Table I). For LLO **1**, two different glycopeptides were identified. The most abundant corresponded to peptide linked to the $GlcNAc_2Man$, according to its molecular weight. The second glycopeptide, for which only a small amount was detected, had a molecular weight coinciding with linked $GlcNAc_2Man_2$, originated from the addition of the first mannose to the LLO by Alg2 (Supplementary Figure 2 and Table I). For LLO analog **2**, glycopeptide containing $GlcNAc_2Man_3$ was the main product, but a significant amount of peptide linked to $GlcNAc_2Man_2$ was also identified (Table I and Supplementary Figure 3). Contrary to Alg1, Alg2 thus displays a minimum length requirement for the lipid tail of the substrate LLO in order to efficiently add both mannoses in vitro. This requirement may be more pronounced for the addition of the α-1,3 mannose, which occurs first and may be the rate-determining step of the double mannosylation reaction.

In order to assess if the α,1–6 branching glycosidic linkage was generated by Alg2, we performed an α,1-2,3 mannosidase digestion of the Man3-containing glycopeptides and analyzed the products by high performance liquid chromatography (HPLC)-MS/MS. We identified $Man_2GlcNAc_2$ linked to peptide as the only product. A separate digestion combining α,1-2,3 and α,1–6 mannosidases led to peptide linked to $ManGlcNAc_2$, which agreed with the formation of and α,1–6 glycosidic bond by Alg2 (Supplementary Figure 4).

The addition of the last two mannoses by $Alg11_{Cyto}$ was performed only for the LLO analogs **3** and **4** (C_{20} and C_{25}, respectively), as shown in Figure 2B. LC–MS/MS analysis showed that the Alg11-catalyzed reaction(s) were highly efficient, as no significant amounts of unreacted substrates or side products were observed (Figure 3 and Supplementary Figure 5), and the molecular weight of the products coincided to peptide linked to $GlcNAc_2Man_5$ (Table I).

Kinetic characterization of the $GlcNAc_2Man_5$ LLO analogs with TbSTT3A

We have earlier described the purification and kinetic characterization of the single-subunit oligosaccharyltransferase TbSTT3A using LLO analogs containing the polyprenyl tails **3** and **4** and a chitobiose glycan moiety (Ramírez et al. 2017). In vivo, TbSTT3A has been observed to show a preference for Dol-PP-$GlcNAc_2Man_5$ over Dol-PP-$GlcNAc_2Man_9$. We now evaluated if the addition of five mannose units to the glycan moiety of the LLO analogs would affect the in vitro activity of TbSTT3A. We analyzed the kinetics of the N-glycosylation reactions using LLO analogs containing one, three or five Mannose units coupled to the polyprenyl tails **3** and **4**. As shown in Figure 4, the LLO-TbSTT3A affinities (analyzed by K_M values) and the glycosylation efficiencies (reflected in k_{cat} values) did not alter significantly for the tested LLO analogs (Table II), indicating that the additional mannose units in the glycan moiety of the LLOs do not affect the in vitro binding to the OST enzyme nor the catalytic step of the glycan transfer reaction.

Discussion

Dol-PP-$GlcNAc_2Man_5$ is an important intermediate LLO in eukaryotic N-glycosylation, because it is the final product of the cytoplasmic part of the biosynthesis and is flipped to the ER lumen for additional glycan transfer. In vitro characterization of proteins involved in the biosynthesis of eukaryotic LLOs has been mostly performed using the native substrates containing the lipid carrier dolichol. Several studies which allowed the identification and characterization of Alg1 (Couto et al. 1984), Alg2 (Yamazaki et al. 1998; O'Reilly et al. 2006; Kämpf et al. 2009) and Alg11 (Cipollo et al. 2001; Absmanner et al. 2010) required the extraction of native substrates and/or products from yeast cells. Even though this approach was proven successful for initial functional studies, it is impractical for structural and detailed kinetic analyses, which require higher solubility and purity as well as larger amounts of substrates. We therefore devised a strategy to generate $GlcNAc_2Man_5$ LLO analogs that could be produced in large amounts and higher purity. The first mannosylation of the synthetic LLO analogs was performed by incubation with the purified cytoplasmic domain of

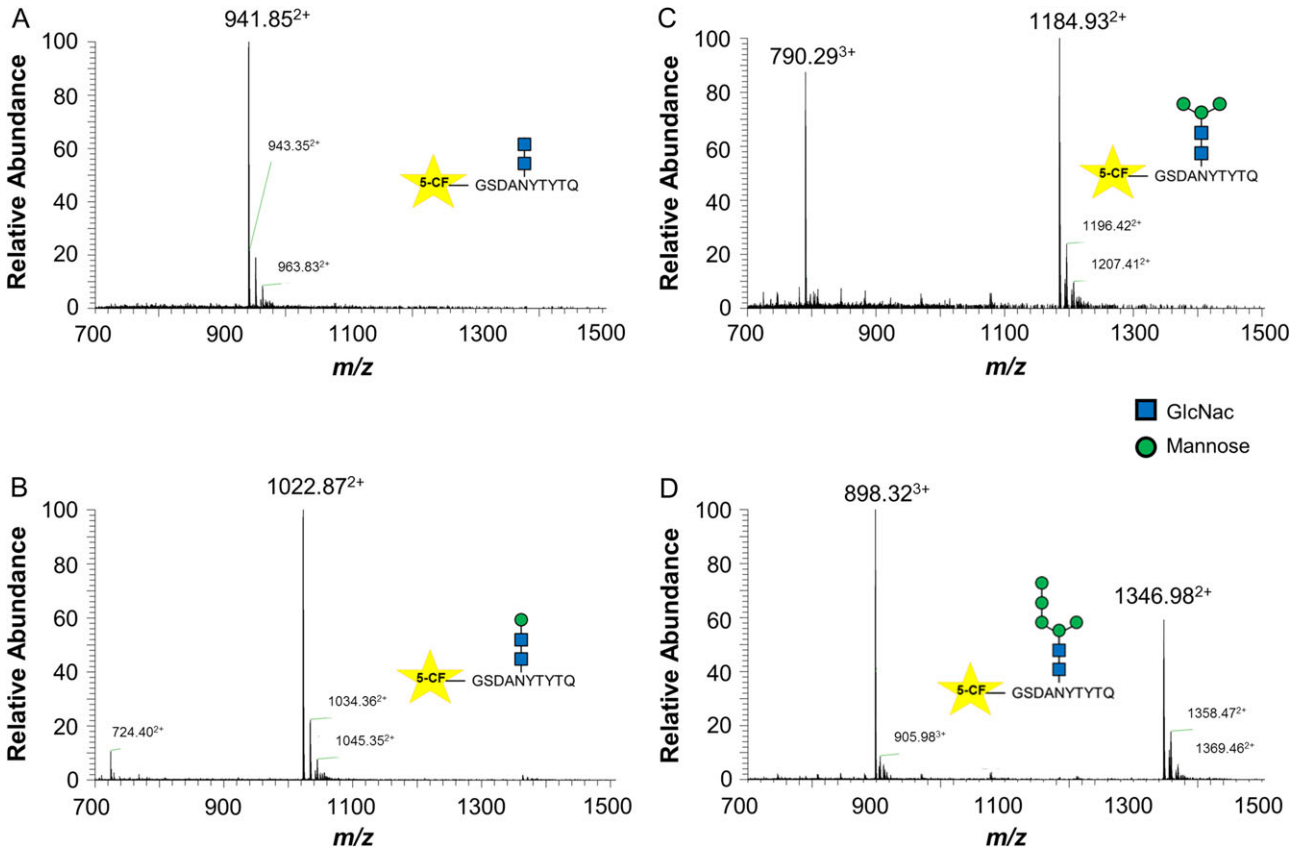

Fig. 3. LC–MS/MS analysis of the glycopeptides generated with the LLO analogs containing glycan moieties of increasing size following processing with Alg proteins. For all reactions, the lipid tail **3** was used. Shown are the MS spectra for the glycopeptides containing chitobiose (**A**) and the products of the sequential addition of mannose residues by Alg1$_{Cyto}$ (**B**), Alg2 (**C**) and Alg11$_{Cyto}$ (**D**). This figure is available in black and white in print and in color at *Glycobiology* online.

Table I. LC–MS/MS analysis of the glycopeptides generated with the LLOs produced by Alg proteins.

LLO analog	Alg reaction	Observed *m/z*	Glycan attached
Citronellyl-PP-Chitobiose (**1**)	Alg1	1022.87^{2+}	$GlcNAc_2Man$
	Alg2	1022.87^{2+}	$GlcNAc_2Man$
		1103.90^{2+}	$GlcNAc_2Man_2$
Farnesyl-PP-Chitobiose (**2**)	Alg1	1022.87^{2+}	$GlcNAc_2Man$
	Alg2	1103.90^{2+}	$GlcNAc_2Man_2$
		1184.93^{2+}	$GlcNAc_2Man_3$
NerylCitronellyl-PP-Chitobiose (**3**)	Alg1	1022.87^{2+}	$GlcNAc_2Man$
	Alg2	1184.93^{2+}	$GlcNAc_2Man_3$
		790.29^{3+}	$GlcNAc_2Man_3$
	Alg11	1346.98^{2+}	$GlcNAc_2Man_5$
		898.32^{3+}	$GlcNAc_2Man_5$
FarnesylCitronellyl-PP-Chitobiose (**4**)	Alg1	1022.87^{2+}	$GlcNAc_2Man$
	Alg2	1184.93^{2+}	$GlcNAc_2Man_3$
		790.29^{3+}	$GlcNAc_2Man_3$
	Alg11	1346.98^{2+}	$GlcNAc_2Man_5$
		898.32^{3+}	$GlcNAc_2Man_5$

LC–MS/MS, liquid chromatography–tandem mass spectrometry; LLO, lipid-linked oligosaccharide.

Alg1, which allowed us to use a single purification step to have highly pure LLO analogs that can be further used for biochemical studies of the reactions involved in the biosynthesis of eukaryotic LLO. Previous reports have shown that an LLO analog containing phytanol coupled to chitobiose could be mannosylated by cell extracts expressing Alg1 or by microsomal fractions from yeast or pig liver (Flitsch et al. 1992; Revers et al. 1994; Wilson et al. 1995). Additionally, the kinetic characterization of the β-1,4 manosyltransferase activity of recombinantly expressed and purified cytoplasmic domain of Alg1 was recently reported (Li et al. 2017). Phytanol is

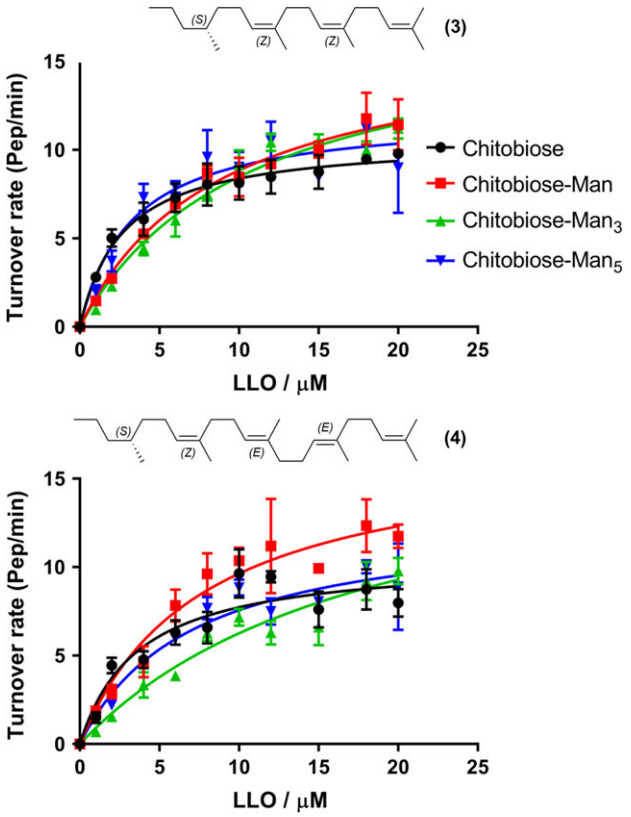

Fig. 4. Kinetic analysis of LLO analogs containing polyprenyl tails (**3**) and (**4**). Glycosylation experiments were performed with 20 nM TbSTT3A protein, 5 μM peptide 5CF-GSDANYTYTQ, 10 mM $MnCl_2$, 150 mM NaCl, 20 mM Hepes pH 7.5, 0.035% *N*-dodecyl-β-D-maltopyranoside (DDM), 0.007% Cholesteryl Hemisuccinate Tris Salt (CHS) and different concentrations of synthetic LLO analogs. Data points reflect the mean of three separate measurements. Error bars indicate standard deviations. Data were fitted by nonlinear regression according to the Michaelis–Menten formula using PRISM. This figure is available in black and white in print and in color at *Glycobiology* online.

Table II. Kinetic analysis of TbSTT3A with the different LLO analogs

LLO analog	K_M (μM)	k_{cat} (pep/min)
(**3**)-PP-$GlcNAc_2$	2.7 ± 0.4	10.6 ± 0.4
(**3**)-PP-$GlcNAc_2Man$	8.8 ± 1.2	16.7 ± 1.3
(**3**)-PP-$GlcNAc_2Man_3$	10.8 ± 1.6	17.6 ± 1.2
(**3**)-PP-$GlcNAc_2Man_5$	3.3 ± 0.8	12.1 ± 0.8
(**4**)-PP-$GlcNAc_2$	3.7 ± 0.9	10.6 ± 0.7
(**4**)-PP-$GlcNAc_2Man$	7.7 ± 1.6	17.0 ± 1.4
(**4**)-PP-$GlcNAc_2Man_3$	18.8 ± 5.0	18.1 ± 2.8
(**4**)-PP-$GlcNAc_2Man_5$	7.1 ± 1.5	12.9 ± 1.1

composed of four saturated isoprenyl units, whereas the lipid carriers we used here have different masses and double bond stereochemistry, showing that the lipid part of the LLO does not have an critical role in the Alg1-catalyzed reaction. There are no biochemical studies of purified Alg2 reported, and all the insight into its activity is derived from studies performed in vivo or with membrane fractions containing Alg2 (Flitsch et al. 1992; Yamazaki et al. 1998; O'Reilly et al. 2006; Kämpf et al. 2009). Our results showed for the first time the activity of purified Alg2 with LLO analogs carrying shorter lipid tails than dolichol. Previously, it was reported that microsome fractions from yeast or pig liver could produce a LLO $GlcNAc_2Man_3$ analog using phytanol-PP-$GlcNAc_2$ as substrate. We found that Alg2 was only active in LLOs carrying the longest oligoprenyl tails (C_{20} and C_{25}), showing that the length of the lipid carrier but not the oxidation state of the lipid moiety was important for the correct function of Alg2 in vitro. This suggests functionally relevant interactions of the lipid tail with the membrane-embedded part of the protein. However, it was shown that truncations of Alg2 are catalytically active in vivo as long as the protein is still associated to the ER membrane by either its N-terminal or C-terminal domain (Kämpf et al. 2009), suggesting that the interaction in the membrane with the LLO substrate is not highly specific. The purification we developed for Alg2 provides an opportunity for future mechanistic studies of the remarkable dual activity of the glycosyltransferase in generating distinct glycosidic linkages.

The two manosylation steps to generate $GlcNAc_2Man_5$ LLO analogs were performed by the purified cytoplasmic domain of Alg11. Similar to Alg1, it had been shown that the N-terminal transmembrane helix of Alg11 is not required for the function of the protein in vivo (Absmanner et al. 2010). Similarly to Alg2, the biochemical characterization of Alg11 had been only performed using the native substrate Dol-PP-$GlcNAc_2Man_3$ (Cipollo et al. 2001; O'Reilly et al. 2006). We now show catalytic activity of Alg11 on LLO analogs with shorter lipid tails.

The LLO analogs we produced accurately represented the different glycan intermediates in eukaryotic LLO biosynthesis and offer advantages for future mechanistic and structural studies, due to the solubility and amounts that can be generated. Specially, analogs of Dol-PP-$GlcNAc_2Man_5$ are of great interest because they can be used as substrates for biochemical studies of at least three different proteins: the flippase that translocates Dol-PP-$GlcNAc_2Man_5$ to the ER lumen, the Alg3 protein that adds the sixth mannose unit in the ER lumen, as well as oligosaccharyltransferases including the single-subunit TbSTT3A (Izquierdo et al. 2009, 2012). Given the in vivo preference of TbSTT3A for Dol-PP-$GlcNAc_2Man_5$ over Dol-PP-$GlcNAc_2Man_9$, it was remarkable that our biochemical characterization of TbSTT3A showed no effect of the glycan length on the apparent affinity of the LLOs. This suggests no specific contact or interaction of these glycan moieties with TbSTT3A. This is analogous to observations obtained with the bacterial oligosaccharyltransferase PglB, where no significant differences were observed in the in vitro activity with the native Und-PP-$BacGalNAc_5Glc$ or its intermediate Und-PP-$BacGalNAc_2$ (Lizak et al. 2014).

Our chemo-enzymatic approach to produce $GlcNAc_2Man_5$ LLO analogs containing lipid carriers with four and five isoprenyl units will not only allow mechanistic and structural studies of the enzymes that use $GlcNAc_2Man_5$ LLOs as substrates, but also represents a first step at exploiting the purified components for the generation of glycoproteins in vitro.

Materials and methods

Cloning, expression and purification of $Alg1_{Cyto}$, Alg2 and $Alg11_{Cyto}$

The gene fragments encoding the cytoplasmic domain of Alg1 (aa 33–349) and Alg11 (aa 46–548) were amplified by PCR using as template previously reported plasmids containing the *ALG1* (Shimma et al. 1997) and *ALG11* (Helenius et al. 2002) genes from *Saccharomyces cerevisiae*, and cloned into a pQE80 (Qiagen, Hilden, Germany) derivative carrying a His10-zz-TEV tag at the N-terminus. The gene encoding human Alg2 was amplified using

cDNA from HEK293 cells as template, and cloned into a modified pUC57 vector carrying His_{10}-YFP tag at the N-terminus.

$Alg1_{Cyto}$ and $Alg11_{Cyto}$ were overexpressed in *E. coli* BL21-Gold (DE3) (Stratagene, San Diego, CA) strain. Cells were grown at 37°C in Luria Bertani medium to A600 nm of 1.0, before expression was induced by the addition of 0.5 mM isopropyl β-D-1-thiogalactopyranoside, for 16 h at 18°C. All following steps were performed at 4°C. Cells were collected by centrifugation, resuspended in lysis buffer (20 mM Tris–HCl, pH 7.5; 150 mM NaCl; 5 mM β-mercaptoethanol; 0.5 mM phenyl- methanesulfonylfluoride) and disrupted by five cycles of sonication (50% amplitude and 50% duty cycle), the cell lysate was incubated with a final concentration of 0.5% Triton X-100, for 1 h. Cell debris and insoluble material were pelleted by ultracentrifugation at 35,000 rpm, in Ti45i rotor, for 30 min. The supernatant was supplemented with 25 mM imidazole and loaded onto a NiNTA superflow affinity column (Qiagen, Hilden, Germany), washed extensively with the same lysis buffer but containing 50 mM imidazole and 0.05% Triton X-100. Elution was performed in the same buffer but containing 200 mM imidazole. The proteins were desalted into 20 mM Tris–HCl, pH 7.5; 150 mM NaCl; 5 mM β-mercaptoethanol and 0.05% Triton X-100 using a HiPrep 26/10 column (GE Healthcare, Little Chalfont, UK).

Expression of Alg2 was performed by transient transfection in human embryonic kidney cells (HEK293), using branched PEI as transfection agent in a 2:1 (w/w) PEI:DNA ratio. After transfection, cells were incubated at 37°C, for 48 h, followed by harvesting and washing with phosphate-buffered saline. Cell pellets were frozen in liquid nitrogen and stored at –80°C until the time of use. For purification, cell pellets were thawed and resuspended in lysis buffer (50 mM Hepes, pH 7.5; 250 mM NaCl; 10% (w/v) glycerol) supplemented with cOmplete™, EDTA-free Protease Inhibitor Cocktail (Roche, Basel, Switzerland). Lysis was performed by dounce homogenization on ice and the cell lysate was incubated with 1% *N*-dodecyl-β-D-maltopyranoside (w/v) (DDM, Anatrace), 0.1% Cholesteryl Hemisuccinate Tris Salt (w/v) (CHS, Anatrace) for two hours at 4°C, then submitted to high-speed centrifugation (35,000 rpm, Ti45i rotor, 30 min). All subsequent buffers contained 0.02% (w/v) DDM, 0.002% (w/v) CHS. The supernatant was loaded onto a Ni/NTA superflow affinity column (Qiagen, Hilden, Germany), washed with the same lysis buffer but containing 50 mM imidazole and eluted with the same buffer but containing 200 mM imidazole. The protein was desalted into 20 mM Hepes, pH 7.5; 150 mM NaCl; 5 mM β-mercaptoethanol, 0.02% DDM and 0.002% CHS, using a HiPrep 26/10 column (GE Healthcare, Little Chalfont, UK).

Chemo-enzymatic synthesis of $GlcNAc_2Man_5$ LLO analogs

The chemical synthesis of the LLO analogs (*S*)-Citronellyl-PP-chitobiose, Farnesyl-PP-chitobiose, (*S*)-NerylCitronellyl-PP-chitobiose and (*S*)-FarnesylCitronellyl-PP-Chitobiose was previously described in detail (Ramírez et al. 2017). All the manosylation reactions were performed in the following buffer (20 mM Tris–HCl, pH 7.5; 150 mM NaCl; 10 mM $MgCl_2$; 5 mM β-Mercaptoethanol and 0.5% Triton X-100). The concentration of the LLO analogs used was in the range of 500 µM to 2 mM.

For the first mannosylation with $Alg1_{Cyto}$, the concentration of GDP-Mannose was adjusted to 2:1 molar ratio (GDP-Man:LLO), and the reaction was incubated at 37°C for 1 h. For the reactions with Alg2 and $Alg11_{Cyto}$ the concentration of GDP-Mannose was adjusted to 4:1 molar ratio (GDP-Man:LLO), and the reactions were incubated over night at 25°C.

The purification of the reaction products was performed by freeze drying of the reaction mixture followed by $CHCl_3$:MeOH (2:1, v/v) extraction. The organic phase was dried in a nitrogen stream and the LLO products resuspended in the reaction buffer or water according to the next step.

The concentration of the different LLO analogs after purification was determined by titrating different amounts of LLOs against a constant amount of the fluorescently labeled acceptor peptide 5CF-GSDANYTYTQ in an in vitro glycosylation assay with TbSTT3A.

Mannosidase digestion of glycopeptides

Digestion of glycopeptides with α,1-2,3 and α,1–6 (NEB, Ipswich, MA) was performed following manufacturer's instructions. The products were analyzed by tricine SDS–PAGE and liquid chromatography mass spectrometry.

In vitro glycosylation assays with TbSTT3A

TbSTT3A was purified as described previously (Ramírez et al. 2017). Reaction mixtures contained 20nM purified TbSTT3A, 10 mM $MnCl_2$, 150 mM NaCl, 20 mM Hepes pH 7.5, 0.035% DDM, 0.007% CHS, 5 µM of the fluorescently labeled acceptor peptide 5CF-GSDANYTYTQ and were incubated with different concentrations of LLO analogs (1–20 µM) for 10 min. Reactions were stopped by the addition of 4X SDS Laemmli buffer and samples were diluted 200-fold prior to analysis by Tricine SDS–PAGE (Schägger 2006). Fluorescent bands for peptide and glycopeptide were visualized by using a Typhoon Trio Plus imager (GE Healthcare, Little Chalfont, UK) with excitation set at 488 nm and using a 526 nm SP emission filter. The amount of formed glycopeptide was determined from band intensities of fluorescence gel scans (ImageJ) (Gerber et al. 2013). Data were fitted by nonlinear regression according to the Michaelis-Menten formula using PRISM software.

Identification of glycopeptides by mass spectrometry

Samples were analyzed on a calibrated Q Exactive mass spectrometer (Thermo Fischer Scientific, Bremen, Germany) coupled to an Thermo Dionex Ultimate 3000 UHPLC system (Thermo Fischer Scientific, Waltham, MA). Kinetex XB-C18 column, 150 × 2.1 mm ID, and 2.6 µm particle size column (Phenomenex, Torrance, CA) were used as the stationary phase. LC mobile phase was composed of two buffer solutions: buffer A was 100% deionized water with 0.1% formic acid (FA) and buffer B was 100% acetonitrile with 0.1% FA. The samples were eluted with a flow rate of 0.3 mL/min by a gradient from 10% to 98% of B in 10 min and back to 10% B in 3 min. The column oven was set to 50°C. Both LC and MS were controlled by XCalibur 2.2 SP1. Data-dependence acquisition (DDA) was first applied to characterize each compound and its corresponding converted product. One scan cycle comprised of a full-scan MS survey spectrum, followed by up to 5 sequential HCD MS/MS with the consideration of theoretical molecular weight of each compound and its corresponding converted product and intense signals above a threshold of 50,000. Both full-scan MS HCD (700–2300 *m/z*) and MS/MS spectra were acquired in the FT-Orbitrap at a resolution of 70,000 at 400 *m/z* for full MS scan and 17,500 for MS/MS scan. HCD was performed by stepped collision energy at 30 V. AGC target values were 3e6 for full FTMS scans and 1e5 for HCD MS/MS scans. Data analysis was performed by XCalibur 3.0 Qual Browser.

Supplementary data

Supplementary data is available at *Glycobiology* online.

Funding

This work was supported by the Swiss National Science Foundation (Transglyco Sinergia program to M.A., J.-L.R. and K.P.L.).

Acknowledgments

We thank the Mass Spectrometry Service (Department of Chemistry and Biochemistry, University of Berne) for recording MS spectra of synthetic substrates.

Conflict of interest statement

None declared.

Abbreviations

CHS, Cholesteryl Hemisuccinate Tris Salt; DDM, *N*-dodecyl-β-D-maltopyranoside; ER, endoplasmic reticulum; FA, formic acid; HPLC, high performance liquid chromatography; LC–MS/MS, liquid chromatography–tandem mass spectrometry; LLO, lipid linked oligosaccharide; MS, mass spectrometry; SDS–PAGE, sodium dodecyl sulphate–polyacrylamide gel electrophoresis.

References

Absmanner B, Schmeiser V, Kämpf M, Lehle L. 2010. Biochemical characterization, membrane association and identification of amino acids essential for the function of Alg11 from Saccharomyces cerevisiae, an alpha1,2-mannosyltransferase catalysing two sequential glycosylation steps in the formation of the l. *Biochem J*. 426:205–217.

Aebi M. 2013. N-linked protein glycosylation in the ER. *Biochim Biophys Acta*. 1833:2430–2437.

Breitling J, Aebi M. 2013. N-linked protein glycosylation in the endoplasmic reticulum. *Cold Spring Harb Perspect Biol*. 5:a013359–a013359.

Burda P, Aebi M. 1999. The dolichol pathway of N-linked glycosylation. *Biochim Biophys Acta*. 1426:239–257.

Cipollo JF, Trimble RB, Chi JH, Yan Q, Dean N. 2001. The yeast ALG11 gene specifies addition of the terminal α1,2-Man to the Man5GlcNAc2-PP-dolichol N-glycosylation intermediate formed on the cytosolic side of the endoplasmic reticulum. *J Biol Chem*. 276:21828–21840.

Couto JR, Huffaker TC, Robbins PW. 1984. Cloning and expression in Escherichia coli of a yeast mannosyltransferase from the asparagine-linked glycosylation pathway. *J Biol Chem*. 259:378–382.

Dell A, Galadari A, Sastre F, Hitchen P. 2010. Similarities and differences in the glycosylation mechanisms in prokaryotes and eukaryotes. *Int J Microbiol*. 2010:148178.

Flitsch SL, Heather Pinches VAL, Taylor JP, Turner NJ. 1992. Chemo-enzymatic Synthesis of a Lipid-linked Core Trisaccharide of N-Linked Glycoproteins. *J Chem Soc Perkin Trans*. 1:2087–2093.

Gao X-D, Moriyama S, Miura N, Dean N, Nishimura S-I. 2008. Interaction between the C termini of Alg13 and Alg14 mediates formation of the active UDP-N-acetylglucosamine transferase complex. *J Biol Chem*. 283: 32534–32541.

Gao X-D, Nishikawa A, Dean N. 2004. Physical interactions between the Alg1, Alg2, and Alg11 mannosyltransferases of the endoplasmic reticulum. *Glycobiology*. 14:559–570.

Gerber S, Lizak C, Michaud G, Bucher M, Darbre T, Aebi M, Reymond J-L, Locher KP. 2013. Mechanism of bacterial oligosaccharyltransferase: in vitro quantification of sequon binding and catalysis. *J Biol Chem*. 288: 8849–8861.

Helenius J, Ng DTW, Marolda CL, Walter P, Valvano MA, Aebi M. 2002. Translocation of lipid-linked oligosaccharides across the ER membrane requires Rft1 protein. *Nature*. 415:447–450.

Izquierdo L, Mehlert A, Ferguson MA. 2012. The lipid-linked oligosaccharide donor specificities of Trypanosoma brucei oligosaccharyltransferases. *Glycobiology*. 22:696–703.

Izquierdo L, Schulz BL, Rodrigues JA, Lucia Güther MS, Procter JB, Barton GJ, Aebi M, Ferguson MA. 2009. Distinct donor and acceptor specificities of Trypanosoma brucei oligosaccharyltransferases. *EMBO J*. 28: 2650–2661.

Jarrell KF, Ding Y, Meyer BH, Albers S-V, Kaminski L, Eichler J. 2014. N-linked glycosylation in Archaea: a structural, functional, and genetic analysis. *Microbiol Mol Biol Rev*. 78:304–341.

Kämpf M, Absmanner B, Schwarz M, Lehle L. 2009. Biochemical characterization and membrane topology of Alg2 from Saccharomyces cerevisiae as a bifunctional α1,3- and 1,6-mannosyltransferase involved in lipid-linked oligosaccharide biosynthesis. *J Biol Chem*. 284:11900–11912.

Kukuruzinska MA, Apekin V, Lamkin MS, Hiltz A, Rodriguez A, Lin CC, Paz MA, Oppenheim FG. 1994. Antisense RNA to the first N-glycosylation gene, ALG7, inhibits protein N-glycosylation and secretion by xenopus oocytes. *Biochem Biophys Res Commun*. 198:1248–1254.

Li S-T, Wang N, Xu S, Yin J, Nakanishi H, Dean N, Gao X-D. 2017. Quantitative study of yeast Alg1 beta-1, 4 mannosyltransferase activity, a key enzyme involved in protein N-glycosylation. *Biochim Biophys Acta*. 1861:2934–2941.

Lizak C, Gerber S, Zinne D, Michaud G, Schubert M, Chen F, Bucher M, Darbre T, Zenobi R, Reymond J-L et al. 2014. A catalytically essential motif in external loop 5 of the bacterial oligosaccharyltransferase PglB. *J Biol Chem*. 289:735–746.

Lu J, Takahashi T, Ohoka A, Nakajima K-I, Hashimoto R, Miura N, Tachikawa H, Gao X-D. 2012. Alg14 organizes the formation of a multiglycosyltransferase complex involved in initiation of lipid-linked oligosaccharide biosynthesis. *Glycobiology*. 22:504–516.

Manthri S, Güther MLS, Izquierdo L, Acosta-serrano A, Ferguson MAJ. 2008. Deletion of the TbALG3 gene demonstrates site-specific N-glycosylation and N-glycan processing in Trypanosoma brucei. *Glycobiology*. 18:367–383.

Nothaft H, Szymanski CM. 2010. Protein glycosylation in bacteria: sweeter than ever. *Nat Rev Microbiol*. 8:765–778.

O'Reilly MK, Zhang G, Imperiali B. 2006. In vitro evidence for the dual function of Alg2 and Alg11: essential mannosyltransferases in N-linked glycoprotein biosynthesis. *Biochemistry*. 45:9593–9603.

Ramírez AS, Boilevin J, Biswas R, Gan BH, Janser D, Aebi M, Darbre T, Reymond J-L, Locher KP. 2017. Characterization of the single-subunit oligosaccharyltransferase STT3A from Trypanosoma brucei using synthetic peptides and lipid-linked oligosaccharide analogs. *Glycobiology*. 27:525–535.

Revers L, Wilson BH, Webberley MC, Flitsch SL. 1994. The potential dolichol recognition sequence of f-1,4-mannosyltransferase not required for enzymic activity using phytanyl-pyrophosphoryl-a-N,N'-diacetylchitobioside as acceptor. *Biochem J*. 299:23–27.

Schägger H. 2006. Tricine–SDS-PAGE. *Nat Protoc*. 1:16–22.

Shimma A, Nishikawa B, bin Kassim Y, Nishikawa A, Kassim B, bin, Eto A, Jigami Y. 1997. A defect in GTP synthesis affects mannose outer chain elongation in Saccharomyces cerevisiae. *Mol Gen Genet MGG*. 256: 469–480.

Takeuchi K, Yamazaki H, Shiraishi N. 1999. Characterization of an alg2 mutant of the zygomycete fungus Rhizomucor pusillus. *Biochim Biophys Acta*. 9:1287–1293.

Wilson IB, Webberley MC, Revers L, Flitsch SL. 1995. Dolichol is not a necessary moiety for lipid-linked oligosaccharide substrates of the mannosyltransferases involved in in vitro N-linked-oligosaccharide assembly. *Biochem J*. 310(Pt 3):909–916.

Yamazaki H, Shiraishi N, Takeuchi K, Ohnishi Y, Horinouchi S. 1998. Characterization of alg2 encoding a mannosyltransferase in the zygomycete fungus Rhizomucor pusillus. *Gene*. 221:179–184.